Chinese Science Bulletin 2003 Vol. 48 No.12 1193—1198

Study of an athermal infrared dual band optical system design containing harmonic diffractive element

SUN Qiang[1,2], WANG Zhaoqi[1], LI Fengyou[1,2], LIU Hongli[1], LU Zhenwu[2], CHEN Bo[2] & MU Guoguang[1]

1. Institute of Modern Optics, Nankai University, Key Laboratory of Opt-electronic Information Science and Technology, Ministry of Education, Tianjin 300071, China;
2. State Key Laboratory of Applied Optics, Changchun Institute of Optics, Fine Mechanics and Physics, Chinese Academy of Sciences, Changchun 130022, China

Abstract **A harmonic diffractive element (HDE) is first successfully introduced to the athermal system of infrared dual band in this paper. In this system, there are only three lens and two materials, silicon and germanium. When the temperature ranges from –70℃ to 100℃ in the dual band, it can simultaneously accomplish the rectification of the longitudinal aberration in the big field of view, as well as the wave front aberration less than 1/4 wavelength. Modulation transfer function of dual band approaches or attains the diffraction limit. The calculation results show that the spectral properties of the HDE are between refractive and diffractive elements, so we can design a simple dual-band and athermal optical system by selecting the thickness and central wavelength of the HDE exactly. Compared with a conventional refractive optical system, this system not only reduces the demand for high technical levels, but also has a compact structure, few elements, a high transmittance better aberrations performances and athermal character. At the same time, the use of the HDE also offers a new element for the infrared optics design.**

Keywords: harmonic diffraction, athermal, infrared dual band, optical design.

DOI: 10.1360/02ww0193

Infrared radiation has three main atmospheric windows, consisting of near infrared (0.75—2.5 μm), midwave infrared (3.2—4.5 μm) and thermal infrared band (8—14 μm). Most infrared optical systems are single band, which causes many insufficiencies in obtaining information. So a dual band imaging optical system has been brought forward by some investigators in order to enhance self-survival and detect targets-enemy[1]. An infrared optical system with dual bands has great superiority in obtaining information, three-dimensional remote sensing, counter- obscure, and adapting performance to various circumstances[2]. Compared with ordinary optical materials, most infrared materials have high optothermal expansion coefficients. With the change of temperature, the refractive index of infrared materials and the dimension and surface shape of optical elements will change. As a result, optical systems cause defocusing, have other aberrations, and the imaging quality will decline. Therefore, many research institutes are searching for an infrared optical system with performance stability and high quality[3]. The performances of athermal infrared optical systems are kept from changing by means of optical passivity, mechanical activity and mechanical passivity in a large temperature range. The structure of optical passivity has been presented by Kanagawa et al.[4—6], which is suitable for the requirement of amodern infrared optical system, due to the low weight and simple structure. So more attention has been paid by scientists. However, these optical refractive systems can correct aberrations only by changing the curvature of surface or using different materials. Therefore, it demands no less than three materials, which are infrared rarity materials, and possesses complex system structures, which results in the debasement of efficiency. Especially at high environmental temperatures, these dual band optical systems could not operate and the quality of images would fall badly.

Hybrid optical systems composed of diffractive and refractive elements, increased the variations in design. Due to the negative chromatic dispersion, diffractive constant and positive power, defocusing results from the optothermal expansion coefficient of materials of elements when temperature variation is consistent with the shift of image plane resulting from the thermal expansion coefficient of the mounting materials, which achieves an excellent athermal effect[7—9].

Dispersion, whereas, is the strongest disfigurement for a usually diffractive imaging lens. The HDE was introduced into optical systems by Sweeney et al. in 1995[10,11], respectively. A single-element diffractive lens with multiwavelength path-length steps has the same optical power for a number of discrete harmonic wavelengths and overcomes the chromatic aberrations of diffractive element to some extent.

In this paper, we investigate an athermal infrared dual band optical system containing a HDE. The given design example is made from two materials (silicon and germanium) and a three-element optical system. It has a large field of view in the 3.7—4.3 and 8.7—11.7 μm regions, and at the same time, the image quality of this system approaches the diffraction limit and has a high optical quality at the temperature range from –70℃ to 100℃, which meets the requirement of the modern hybrid dual band athermal infrared optical system.

1 Theory of athermal infrared dual band system with HDE and refraction

(i) Theory of HDE. For the HDE, the phase jumps at the zone boundaries and can be taken as $p\lambda_0$, where p is an integer ($\geqslant 2$), i.e. the design wavelength is $p\lambda_0$ and the focus length is f_0, which is equivalent to the conventional refractive lens as shown in Fig. 1. So there is an infinite number of focal lengths $f_{m,\lambda}$, given by $\frac{p\lambda_0}{m\lambda}$. It is interesting to note that when $f_{m,\lambda}$ is equal to unity, several wavelengths within a given band come to a common focus f_0, which can be written as $\lambda m = p\lambda_0$, where p is a designed parameter and it offers a mechanism to control specific wavelengths in a given band or bands that will come to a fixed focus. The power of band 1 and band 2 of a harmonic diffractive surface is respectively given by $\frac{kp\lambda_1}{m_1}$ and $\frac{kp\lambda_2}{m_2}$, where k is a constant, corresponding to the radius, magnitude and the period number of the zone. The dispersion power of harmonic diffraction over band 1 (mid-infrared band) and band 2 (thermal infrared band) is respectively given by

$$V_1 = \frac{\lambda_{(1)\text{mid}}}{\lambda_{(1)\text{short}} - \lambda_{(1)\text{long}}}, \tag{1}$$

$$V_2 = \frac{\lambda_{(2)\text{mid}}}{\lambda_{(2)\text{short}} - \lambda_{(2)\text{long}}}. \tag{2}$$

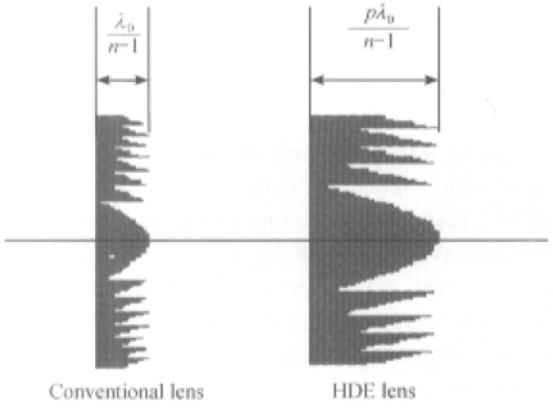

Fig. 1. Sketch of HDE compared with the conventional lens.

We can determine the original system structure based on the distribution of total power, and design the power, radius, magnitude of zone, and the period number of zone of the harmonic diffractive surface after the optimizition by ZEMAX software.

(ii) Theory of the infrared athermal system of a dual band with refractive/diffractive elements. For a refractive lens, aberrations of the optical system are high-order minimum of the focus. The temperature has complicated effects on aberrations, but mostly on defocusing. We can calculate the amount of defocusing due to the change of temperature, by derivation calculus. Whether in a single-element lens or in set of lens, the amount of defocusing depends on the refractive index and the thermal expansion coefficient of the materials used in the system, which is independent of the surface curvature of the element. When the temperature is T and the radius is r, the phase distribution of elements can be expressed as eq. (3):

$$\Phi r(r) = \sum_{i=1}^{N} A_i(T) r^{2i}. \tag{3}$$

Then the relationship between the coefficients of phase polynomials of the binary element and temperature can be described by eqs. (4) and (5) (the coefficients of higher orders have little effect on the system, so we only use the first two coefficients here):

$$\frac{\mathrm{d}A_1}{\mathrm{d}T} = -2(\alpha_g A_1), \tag{4}$$

$$\frac{\mathrm{d}A_2}{\mathrm{d}T} = -4(\alpha_g A_2). \tag{5}$$

From the above equations, we can see that the relations are very simple. They only depend on the thermal expansion coefficients of the materials, and have no relation to the refractive index. The variation of the refractive index only affects the equivalent depths of the surface steps in the element, i.e. it affects the diffraction efficiency. In fact, the effect can be neglected because of the small change refraction index. Here, A_1 shows the power of the binary element, A_2 shows the spherical aberration. For the infrared wide-band system, A_2 is much less than A_1, so the change of temperature mostly affects the defocusing of the binary element, which has little effect on higher spherical aberration and other higher aberrations. All the refractive elements and binary elements in the system will induce defocusing. The thermal expansion coefficients of the refractive elements made from the materials of silicon and germanium are positive, so they will induce some positive power. However, the thermal expansion coefficients of the binary elements are negative, and they will induce some negative power. Though the thermal expansion coefficient of the binary element is less than that of the refractive element, we can control the binary element contribution to the power by controlling the dimension of the cycle and the number of the rings, and the defocusing of the binary element. So we can make clear that the defocusing in the mid-infrared band and the thermal infrared band of the system correspond to the shift of the image plane due to the thermal expansion of mounting materials respectively.

The athermal dual band system should keep the im-

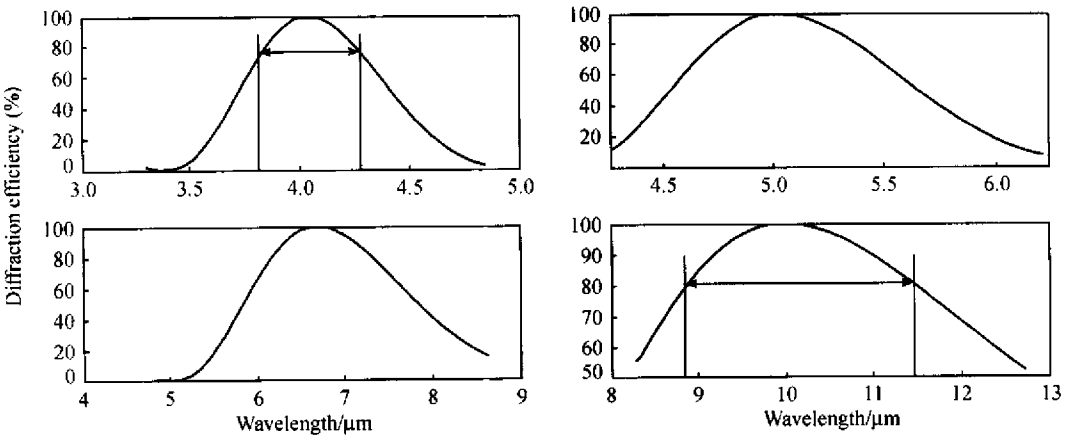

Fig. 2. The diffraction efficiency of harmonic wavelength at $p = 2$ (the harmonic wavelength is 10, 6.7, 5 and 4 μm, respectively).

age planes of different wavelength bands on the same plane, and keep the numerical aperture from changing. At the same time, it should make the quality of image meet the requirement. In this paper, we designed one three-element system with harmonic diffraction, which used only two materials, silicon and germanium. It should satisfy the distribution of power and the equation of weakening longitudinal color aberration and athermal equation, so we can obtain the parameters of the system in dual bands according to these three equations.

2 Example of design of HDE

To illustrate the spectral characteristics of a harmonic diffractive lens over mid-infrared and thermal infrared, a harmonic diffractive lens was designed for operation at $p = 2$ and $m = 2, 3, 4, 5$ based on the HDE theory, i.e. the harmonic wavelength is 10, 6.7, 5 and 4 μm, respectively. The design central wavelength was 10 ($\lambda_0 =$ 10 μm). We calculated the diffraction efficiency of the harmonic wavelength using the Matlab software based on the expression of eq. (6) as shown in Fig. 2.

$$\eta_m = \left[\frac{\sin\left\langle \pi\left\{ \frac{\lambda_0}{\lambda}\left[\frac{n(\lambda)-1}{n(\lambda_0)-1} \right] p - m \right\} \right\rangle}{\pi\left\{ \frac{\lambda_0}{\lambda}\left[\frac{n(\lambda)-1}{n(\lambda_0)-1} \right] p - m \right\}} \right]^2 . \quad (6)$$

From Fig. 2 we can see that the wave bands of the diffraction efficiency around central wavelength of 6.7 and 5 μm are not the infrared windows, so the both harmonic diffractive wavelengths are not calculated for the system design. However, the wave bands of the diffraction efficiency around the central wavelength of 10 and 4 μm are in the spectral regions of thermal infrared and mid-infrared. The spectral regions in which diffractive efficiency is calculated to be 80% act as an operational band in the infrared system using the harmonic order of $m = 2$ and $m = 5$. The concrete parameter of the system including three elements are chosen as follows: work wavelength range: band 1 is 3.7—4.3 μm, and band 2 is 8.7—11.5 μm; the total field of view (2*FOV) is 3°; the effective focal length (EFL) is 71 mm; system aperture is 30 mm; the shell of system is made from aluminium. The power of HDE is very small and HDE is located in the rear of the third lens. So we calculate the power and original structure of the system after supposing the power of the HDE to be zero.

Because the power of the system, surface structure, and thickness are all confirmed, the refractive index of the materials selected should be near to the supposed curves slopes at the corresponding wavelength over the mid-infrared and thermal infrared bands, in order to accomplish imaging and correcting aberrations in two bands simultaneously. Fig. 3 shows the schematic diagram of selected favourable materials.

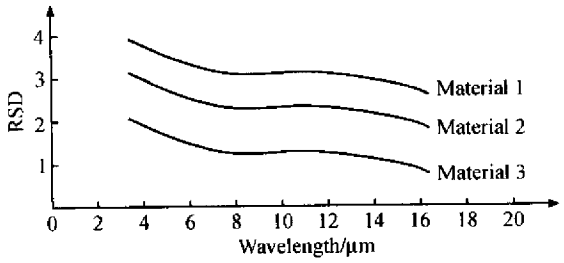

Fig. 3. Schematic diagram of selected favourable materials (The RSD represents the ratio of refractive index to wavelength).

Thus, with the properties of the harmonic diffractive surface about correcting color aberrations, we can weaken aberrations well in every wave band. According to refs. [12] and [13], we selected silicon and germanium as mate-

rials. Introducing the harmonic diffractive surface into the system, we treated the data by ZEMAX software. The distribution of power and the position of every lens are adjusted again by calculation of ZEMAX software, which has the function of "the effect on temperature changing to system". At last, the structure of the system could be determined by optimizing and calculating the phase structure of HED using the optimized function. Fig. 4 shows the structure of the whole system. The 4th and the 5th planes are high order aspherical planes, which are beneficial to correct the spherical and coma aberrations. The 6th plane is a harmonic diffractive plane.

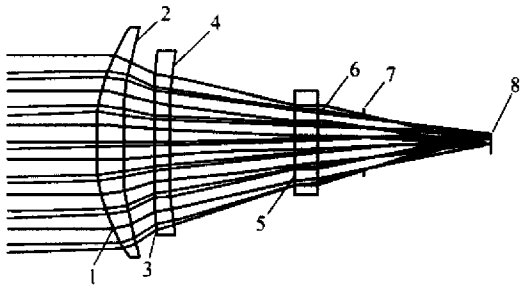

Fig. 4. Structure of the athermal optical system for the infrared dual band. 1—5 represent the number of the surface of lenses, 6 is the harmonic diffractive plane, 7 is the cool pupil and 8 the image plane.

Figs. 5 and 6 show the modulation transfer function (MTF) (near to diffraction limit at 50 line pairs) and the transverse ray aberration (the maximum value is 0.065 mm) of the system at −70℃ in the mid-infrared band. Figs. 7 and 8 show the MTF (near to diffraction limit at 50 line pairs) and transverse ray aberrations (the maximum value is 0.07 mm) of the system at 100℃ in the mid-infrared band. Figs. 9 and 10 show the MTF (near to the diffraction limit at 50 line pairs) and transverse ray aberration (the maximum value is 0.11 mm) of the system at −70℃ in the thermal infrared band. Figs. 11 and 12 show the MTF (near to the diffraction limit at 50 line pairs) and transverse ray aberration (the maximum value is 0.09 mm) of the system at 100℃ in the thermal infrared band.

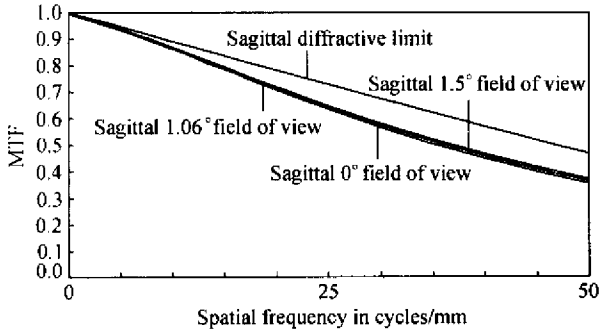

Fig. 5. The MTF layout of mid-infrared band at −70℃.

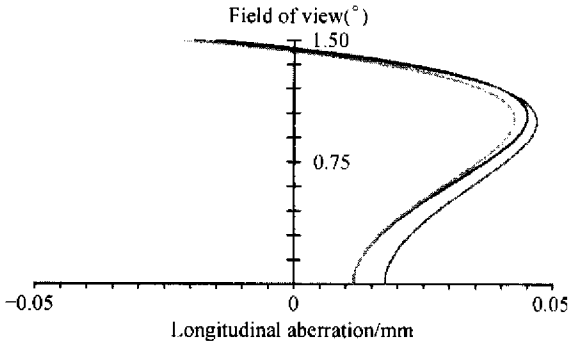

Fig. 6. The longitudinal aberration layout of mid-infrared band at −70℃.

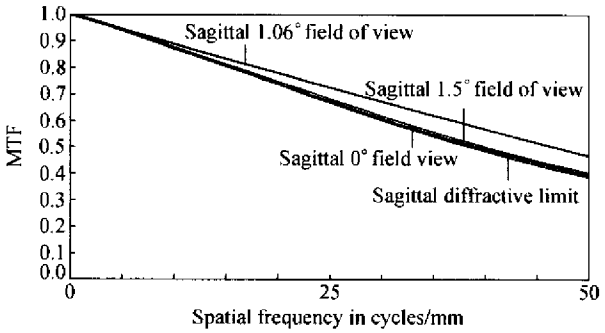

Fig. 7. The MTF layout of mid-infrared band at 100℃.

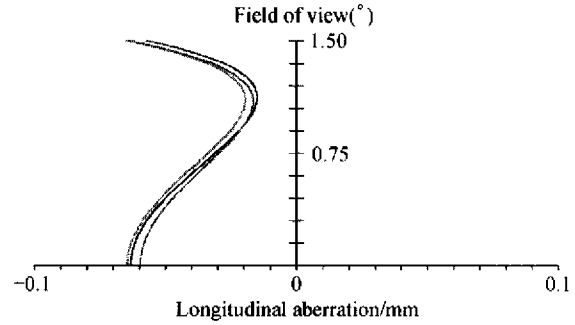

Fig. 8. The longitudinal aberration layout of mid-infrared band at 100℃.

The relationship of the wave front and temperature in two wavebands has also been given in Fig. 13. From Fig. 13, we can see that the wave front aberrations of the system in two bands in the temperature range from −70℃ to 100℃ are all less than 1/4 λ_0 . This indicates that the defocusing is less than the focus length. That is, the largest difference between the practical and the ideal plane does not exceed 1/4 λ_0 . The wave surface is considered without defect, and the MTF approaches the diffraction limit, so this hybrid optical system can be used practically. However, we can also see that the aberration performances are better in the thermal infrared band. The reason is

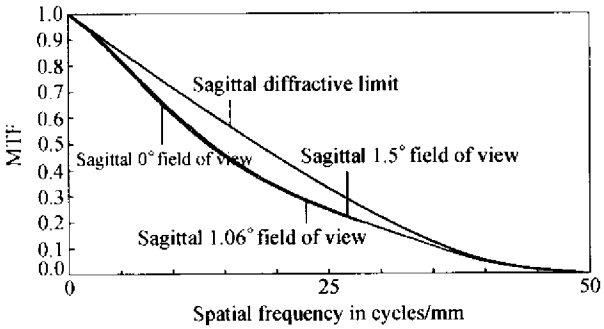

Fig. 9. The MTF layout of thermal infrared band at −70℃.

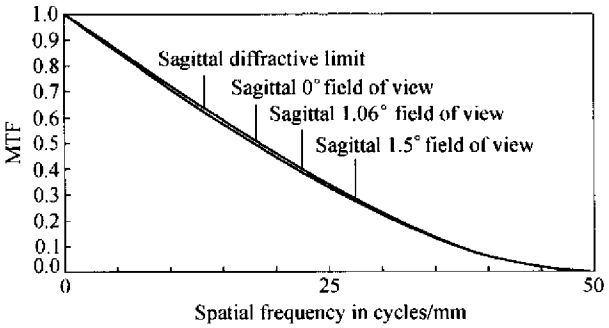

Fig. 11. The MTF layout of thermal infrared band at 100℃.

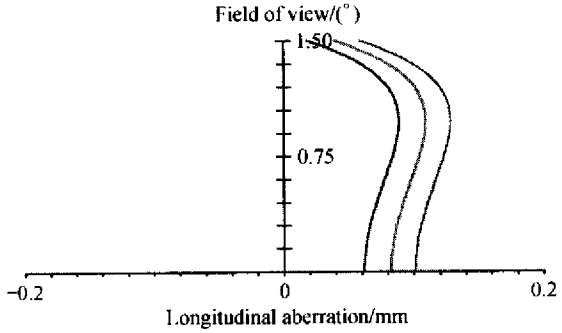

Fig. 10. The Longitudinal aberration layout of thermal infrared band at −70℃.

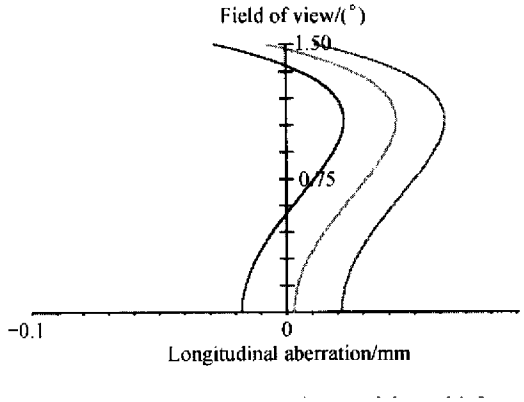

Fig. 12. The longitudinal aberration layout of thermal infrared band at 100℃.

that central wavelength is 10 μm, the others are harmonic wavelengths, and the wave band of the given diffraction efficiency becomes narrow with the diffraction order increasing, which makes the diffractive efficiency decrease. Furthermore, the ratio of the slopes of three chords over their respective wavebands approach the slopes of the supposed curve only in the thermal infrared band but not in the mid-infrared, i.e. it cannot satisfy the system requirements.

3 Conclusions

In this paper, an infrared dual band athermal system was designed by using HDE, selecting silicon and germanium, and the most simple infrared materials.

The HDE can obtain the same power in a series of discrete wavelengths. With the design parameter p increasing, the thickness of the HDE increases, and the shape of HDE gradually trends to the refractive lens. Dispersion lies between the refractive and diffractive lenses, which can overcome the defect of the larger dispersion of the diffractive element to some extent. Moveover, the thermal expansion coefficients of diffractive elements are opposite to those of the most infrared materials, and independent of the refractive index temperature coefficients of most materials. Based on the window characteristics of the infrared bands and the properties of the thermal expansion coefficients of the diffractive elements, we can introduce HDE into the infrared of the dual band athermal system successfully by selecting the appropriate parame-

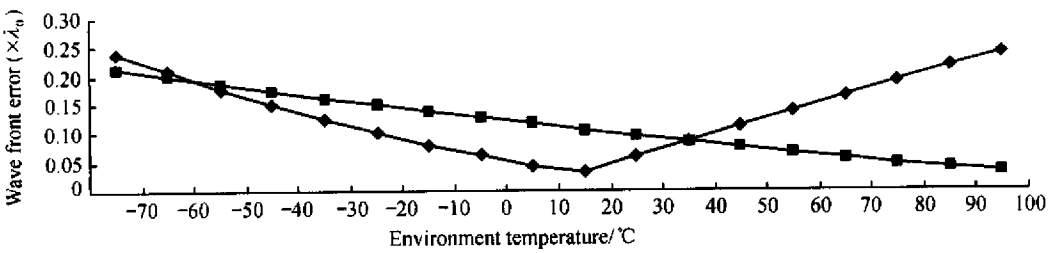

Fig. 13. The relation sketch between the wave front and temperature. ◆, Curve in mid-infrared band; ■, curve in thermal infrared band.

ter p and central wavelength λ_0.

So a dual band athermal system with HDE can not only satisfy the requirements of correcting and athermal aberrations in dual bands simultaneously, but also achieve the compact structure with few elements and a high transmittance. Moreover, the overall system has low weight, a small volume, a wide work temperature range, a flat diffractive plane and a big character size, which makes the system function easily. At the same time, the system has better aberration performances, provides imaging qualities near the diffraction limit over a wide field of view, offers a new component for optics designs based on HDE, relaxes the demand for the high technical level, and can be used in a dual band or multi-band optical imaging systems with a wide field of view and larger numerical aperture. Therefore, HDE possesses great value in many aspects, such as athermal design, correcting color aberrations, zoom systems, etc., which benefits the development of military and civilian technologies.

Acknowledgements This work was supported by the State Key Laboratory of Applied Optics, Changchun Institute of Optics and Fine Mechanics and Physics (Grant No. 60277021), and Joint Academy of Nankai University and Tianjin University.

References

1. Wu Zongfan, Liu Meilin, Zhang Shaoju et al., Infrared Technology (in Chinese), Beijing: National Defence & Industry Press, 1998, 286—300.
2. Jamieson, T. H., Ultrawide waveband optics, Opt. Eng., 23(2): 111—116.
3. Guo Yonghong, Shen Mangzuo, Lu Zukang, Design for infrared diffractive/refractive optical system, Acta Optical Sinica (in Chinese), .2000, 20(10): 2392—2395.
4. Kanagawa, Y., Wakabayashi, S., Tiajime, T. et al., Expansion of an athermal chart into a multilens system with thick lenses spaced apart, Opt. Engng., 1996, 35(10): 3001—3006.
5. Jamieson, T. H., Thermal effects in optical systems, J. Opt. Soc. Am., 1948, 38: 542—546.
6. Kanagawa, Y., Wakabayashi, S., Tiajime, T. et al., Multilens system design with an athermal chart, Appl. Opt., 1994, 33(34): 8009—8013.
7. Wood, A. P., Design of infrared hybrid refractive-diffractive lenses, Appl. Opt., 1992, 31(13): 2253—2258.
8. Stone, T. George, N., Hybrid diffractive-refractive lenses and achromats, Appl. Opt., 1988, 27(12): 2960—2971.
9. Tamagawa, Y. Tajime, T., Dual-band optical systems with a projective athermal chart: Design. Appl. Opt., 1997, 36(1): 297—301.
10. Sweeney, D. W., Gary, E., Sommargren, harmonic diffractive lenses, Appl. Opt., 1995, 34(14): 2469—2475.
11. Faklis, D., Morris, G. M., Spectral properties of multiorder diffractive lenses, Appl. Opt., 1995, 34(14): 2462—2468.
12. Li Shixian, Li Lin, Manual of Optical Design (in Chinese), Beijing: Beijing Technology University Press, 1995, 69—116.
13. Yuan Xucang, Optical Design (in Chinese), Beijing: Beijing Technology University Press, 1988, 96—143.

(Received December 30, 2002)

Chinese Science Bulletin 2003 Vol. 48 No.12 1198—1200

Violet/blue photoluminescence from CeO_2 thin film

CHAI Chunlin, YANG Shaoyan, LIU Zhikai, LIAO Meiyong & CHEN Nuofu

Key Laboratory of Semiconductor Material Science, Institute of Semiconductors, Chinese Academy of Sciences, Beijing 100083, China

Abstract **CeO_2 thin film was fabricated by dual ion beam epitaxial technique. The violet/blue PL at room temperature and lower temperature was observed from the CeO_2 thin film. After the analysis of crystal structure and valence in the compound was carried out by the XRD and XPS technique, it was inferred that the origin of CeO_2 PL was due to the electrons transition from Ce*4f* band to O*2p* band and the defect level to O*2p* band. And these defects levels were located in the range of 1 eV around Ce*4f* band.**

Keywords: cerium dioxide thin film, PL, violet/blue.

DOI: 10.1360/02ww0200

CeO_2 is a rare-earth oxide which has a face centered cubic fluorite crystal structure. It has fine chemical stability and high dielectrics (ε = 26). Its lattice constant has closely matched to silicon and the dismatch is about 0.35%. It is always investigated as insulator material in the silicon-on-insulator (SOI) structures, dielectric material and the buffer layer between the superconductor $Yba_2Cu_3O_7$ and the Si substrate[1—6]. Recently, the PL of CeO_2 was studied by many groups. The PL from CeO_2 through annealing at 1100℃ was investigated by Morshed in 1997[7]. They thought the peak at 400 nm resulted from the formation of new phase Ce_6O_{11} in the crystal. In 1999, Choi[8,9] observed the PL peak centered at 358 nm and its origin was from $Ce_2Si_2O_7$ phase. The green PL[10] was obtained in 2001, and its origin was from the $Ce(OH)_4$ forming at the interface. In this report, the PL of the CeO_2 as grown was studied at room temperature and lower temperature. It is inferred that the PL is related to the location of oxygen defect level after being studied using the XPS and XRD technique.

1 Experiments

CeO_2 thin film was grown by dual ion beam epitaxial technique, and the detailed introduction about the deposition system is shown in ref. [11]. N-type Si(100) wafers with 2—4 Ω • cm resistivity were used as substrates. The silicon, which was cleaned with ethanol, acetone, HF acid and deionized water, was delivered into the deposition chamber by mechanical hand. The vacuum pressure was less than 1×10^{-6} Pa in the chamber. Both ion beams were produced by Bernas-type and Freeman-type ion source. Through mass-selection in magnetic filed and accelerating